Hybrid Quantum–Classical Convolutional Neural Network for Robust RF Sensing

†Yujie Sun, ‡Xuyu Wang, and †Shiwen Mao
†Department of Electrical and Computer Engineering, Auburn University, Auburn, AL 36849-5201
‡Knight Foundation School of Computing and Information Sciences, Florida International University, Miami, FL 33199
Email: yzs0124@auburn.edu, xuywang@fiu.edu, smao@ieee.org

***Abstract*—Recent advances in quantum machine learning have motivated the exploration of quantum neural network (QNN) for sensing and signal processing tasks. In this paper, we propose a hybrid quantum–classical neural network framework for RF sensing, designed to address the challenges of noise, non-linearity, and complex spatio-temporal dependencies in RF signals. In our approach, RF time-series measurements are encoded into quantum states and processed by parameterized quantum circuits to perform convolution-like operations, while a classical classifier produces the final predictions. Overall, this work highlights the potential of QNN to enhance accuracy, parameter efficiency, and robustness in wireless sensing, and suggests a promising direction for next-generation RF sensing activity recognition and cross-domain sensing applications.**

***Index Terms*—Quantum Neural Network, Human Activity Recognition, RF Sensing.**

I. Introduction

In recent years, convolutional neural network (CNN) have achieved remarkable success in computer vision [1], natural language processing [2], and wireless sensing [3]. However, their performance is often constrained when dealing with highly structured and noisy data such as RF sensing signals [4]. RF sensing datasets typically consist of multi-dimensional and time-varying channel state information (CSI), which exhibits non-linear dependencies, phase noise, and missing values. Classical CNNs require extensive preprocessing and large-scale training data to capture these complex patterns, while their computational complexity and reliance on parameter scaling further limit generalization. Quantum computing has emerged as a promising paradigm, offering intrinsic parallelism and entanglement that can potentially accelerate feature extraction and improve robustness in learning from noisy RF sensing signals [5], [6].

Recent advances in quantum machine learning [7] have motivated the development of hybrid architectures that integrate classical neural network with parameterized quantum circuits. Among these, the quantum neural network (QNN) proposed by Cong [8] stands out as an elegant quantum analogue of classical CNNs. QNN employs local quantum gates to mimic convolutional operations and uses qubit reduction or measurement as pooling, thereby enabling hierarchical feature extraction on quantum states [9], [10]. These models have demonstrated effectiveness in quantum phase recognition, entanglement detection, and small-scale image classification, suggesting that convolutional principles can be generalized to quantum systems [11].

The potential advantage of QNN lies in their unique ability to exploit quantum entanglement and superposition, which allows them to represent complex correlations in high-dimensional data more compactly than their classical CNN counterparts [12]. Unlike classical convolutions that rely on large numbers of filters and parameters to capture local dependencies, QNN can encode global correlations across qubits with significantly fewer resources, thereby reducing model size without sacrificing expressive power [13]. This property is particularly beneficial for RF sensing datasets [14], [15], which are inherently noisy, non-linear, and often incomplete due to signal attenuation, interference, and missing samples. Traditional CNNs typically require heavy preprocessing pipelines and extensive parameter tuning to handle such imperfections, while QNN can naturally leverage quantum correlations to enhance resilience against uncertainty. By achieving efficient feature compression and maintaining robustness in the presence of noise, QNN offer a promising new direction for advancing wireless sensing tasks [16], [17]. More broadly, they provide a pathway toward scalable models that can overcome the limitations of classical approaches in terms of both generalization across domains and adaptability to diverse real-world conditions [18].

In this paper, we present a comprehensive study of QNN for RF sensing tasks. Unlike prior works that mainly focused on applications in quantum many-body physics or small-scale synthetic datasets, our work is among the first to systematically extend QNN to real-world RF sensing data, which are inherently characterized by measurement noise, non-linear dependencies, and missing values. By tackling these challenges, we aim to evaluate whether QNN can provide a scalable and robust alternative to classical CNNs in practical sensing scenarios. The main contributions of this paper can be summarized as follows:

- We design a hybrid QNN architecture tailored for RF sensing datasets, incorporating efficient quantum convolution and pooling modules for hierarchical feature extraction.
- We systematically evaluate QNN against classical CNNs and other baselines, highlighting their advantages in parameter efficiency, robustness to noise, and scalability.
- We investigate how QNN handle the unique challenges of

RF sensing data, providing empirical evidence and theoretical insights into their potential for broader wireless sensing applications. engineering strategy.

We next present the motivation and problem formulation in Section II, followed by our system design in Section III. We discuss our experimental setup and analysis results in Section IV. Section V concludes this paper.

II. Motivation and Problem Formulation

In RF sensing-based human activity recognition, a set of N transmitters, receivers, or passive devices is deployed to capture human motions through variations in reflected or backscattered RF signals. The transmitter emits RF probing signals, and the receivers collect the corresponding responses. Depending on the sensing modality, the recorded measurements may include amplitude, phase, or full CSI over time, thereby forming a time-series representation of human activities.

By stacking these responses over an observation window of length T, we obtain a two-dimensional matrix $X \in \mathbb{R}^{T\times N}$, where each row corresponds to a time step and each column corresponds to one sensing dimension. This representation captures both the temporal dynamics and the spatial distribution of RF sensing signals, and is later divided into local patches for quantum encoding and convolution.

Despite recent advances, modeling RF sensing data remains highly challenging. The multi-antenna and multi-subcarrier responses are often distorted by multipath interference, low signal-to-noise ratio (SNR), phase wrapping, and frequent missing samples. Furthermore, discriminative patterns are nonlinear and distributed across time, frequency, and antenna domains, making them difficult to capture using conventional methods. Classical deep learning models such as CNNs and recurrent neural networks (RNNs) have achieved progress in RF sensing tasks, but they generally require extensive preprocessing pipelines, large amounts of labeled data, and heavy parameterization. In fact, their generalization ability is limited under domain shifts caused by variations in users, locations, or environments. These challenges call for new approaches that can represent RF data more compactly, handle uncertainty more effectively, and generalize better across diverse conditions.

The objective of RF sensing-based HAR is to learn a mapping function $f : \mathbb{R}^{T\times N} \to \{1, 2, \ldots, C\}$ that classifies each activity instance into one of C predefined categories. While shallow models such as support vector machines (SVMs) with handcrafted features can handle simple cases, their performance degrades substantially in complex, high-dimensional, and cross-domain scenarios. To address these challenges, we propose a hybrid quantum–classical framework that integrates quantum convolutional feature extraction with a classical classification head. By leveraging quantum entanglement and superposition, the proposed framework aims to achieve robustness, scalability, and superior representation learning in RF sensing.

III. System Design

A. Overview

Our framework adopts a hybrid quantum–classical architecture to address the challenges of RF sensing. The overall pipeline consists of four interconnected modules: input representation, quantum convolution, quantum pooling and feature compression, and classical classification, which together form an end-to-end sensing and recognition system.

In the input representation stage, raw RF measurements are organized into fixed-length observation windows and partitioned into local spatio-temporal patches. This step captures localized dynamics in time and frequency domains, providing structured inputs to the quantum model.

In the quantum convolution layer, each local patch obtained from the preprocessed RF data is encoded into quantum states using Hadamard and parameterized rotation gates. Entangling operations are then applied across qubits to capture high-order local correlations, analogous to convolution kernels in classical CNNs.

The quantum pooling and feature compression stage measures the quantum states in the Pauli-Z basis. This step produces compact feature representations, effectively reducing the dimensionality of the input while retaining discriminative information. The process plays a role similar to pooling in classical networks, but leverages quantum measurement to provide parameter-efficient compression.

Finally, in the classical classification head, the compressed quantum features are aggregated and passed into a fully connected neural network. This stage performs the final classification into C activity classes, providing robust nonlinear decision boundaries and ensuring scalability under noisy and heterogeneous sensing conditions.

B. Input Representation and Data Encoding

In RF sensing-based human activity recognition, the raw data is collected as time-varying measurements across multiple antennas, subcarriers, or tags. Formally, each activity instance can be represented as a two-dimensional matrix $X \in \mathbb{R}^{T\times N}$, where T is the number of discrete time steps in the observation window and N is the number of sensing dimensions (e.g., antennas, subcarriers, or tags, depending on the modality). Each column of X corresponds to the temporal response of one sensing dimension, while each row corresponds to the responses of all dimensions at a specific time step. This representation captures both the temporal dynamics and the spatial distribution of RF sensing signals.

To make the data suitable for quantum processing, we partition the matrix X into local patches of size $V \times W$ using a sliding window with stride s. This step mirrors the receptive field concept in classical convolutional networks, allowing local spatio-temporal dependencies to be modeled hierarchically. Each patch is then flattened into a vector $p \in \mathbb{R}^{VW}$, which serves as the input to the quantum encoding stage.

C. Quantum Convolution Layer

In classical deep neural network, convolutional layers extract local spatial or temporal correlations from input feature maps through sliding windows, while weight sharing and pooling operations enable parameter compression and feature abstraction. However, RF sensing data often exhibits strong nonlinearity, cross-domain dependencies, and complex noise interference, which limit the ability of classical convolutions to capture high-order correlations and handle uncertainty effectively.

To address this, we introduce the Quantum Convolution Layer. In this layer, each local input patch is mapped into a quantum state and processed by a parameterized quantum circuit consisting of rotation and controlled gates. These operations exploit quantum superposition to capture diverse feature patterns and leverage entanglement to model high-order correlations. As illustrated in Fig. 1, input features are encoded into qubits using RY rotations, entangled with CRZ gates, and measured in the Z basis to produce compact quantum features. This design mirrors classical convolution kernels while exploiting quantum effects for more expressive and parameter-efficient feature extraction.

Specifically, given a local vector $p \in \mathbb{R}^{VW}$ (obtained by flattening a $V \times W$ patch), we first embed it into n qubits using amplitude encoding or angle encoding. The quantum circuit then applies a sequence of trainable single-qubit rotation gates and multi-qubit entangling gates, serving as the equivalent of convolutional filters. Through multiple quantum operations, the latent correlations of the input patch are encoded into the amplitudes or phases of the quantum state. Finally, measurement in the computational basis yields a low-dimensional classical vector, which is used for subsequent feature aggregation and classification.

Compared with classical convolutional layers, the quantum convolutional layer achieves parameter efficiency, since the number of quantum gates grows only logarithmically with circuit depth, resulting in far fewer parameters than classical convolutional kernels. It also provides enhanced expressivity, as quantum superposition and entanglement naturally capture complex nonlinear relationships across time, frequency, and spatial domains. Moreover, it demonstrates improved robustness, because quantum features are able to preserve discriminative information under noise and domain shifts, thereby helping to mitigate overfitting. Therefore, the quantum convolutional layer can serve as an alternative or complementary module to classical CNNs, offering more compact and robust feature extraction for RF sensing tasks.

D. Quantum Pooling and Feature Compression

Following quantum convolution, the feature representation remains high-dimensional, as each local patch contributes an n_{qubits}-dimensional vector. To reduce redundancy and enforce hierarchical abstraction, we employ a quantum pooling mechanism that parallels downsampling in classical CNNs. In our design, pooling is realized through selective measurement and qubit reduction. Specifically, a subset of qubits is chosen

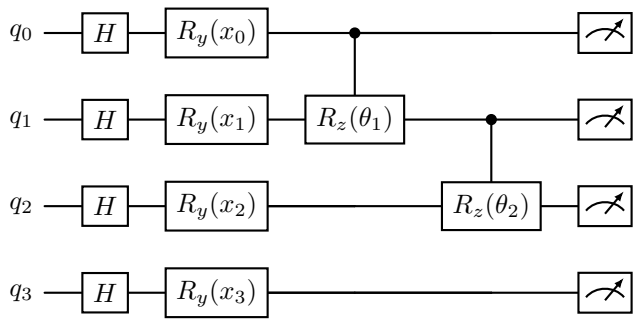

Figure 1: An example of a 4-qubit quantum convolutional layer in QNN. Each input patch is first encoded with Hadamard and R_y rotations, followed by controlled-R_z gates for entanglement. Finally, measurements in the Z basis provide features for subsequent processing.

for measurement in the Pauli-Z basis, and their expectation values are retained as compressed features. The remaining qubits are either discarded or reset, effectively reducing the number of active qubits and compressing the quantum state representation. This process acts as a dimensionality reduction step, eliminating redundant information while preserving the most discriminative correlations.

Formally, given a post-convolutional state $|\psi'\rangle$ encoded on n_{qubits} qubits, the pooling operation selects a subset $\{i_1, i_2, \ldots, i_m\} \subseteq \{1, \ldots, n_{qubits}\}$ with $m < n_{qubits}$, and computes

$$p_j = \langle \psi' | Z_{i_j} | \psi' \rangle, \quad j = 1, \ldots, m.$$

The resulting feature vector $\mathbf{p} \in \mathbb{R}^m$ serves as the pooled representation for the corresponding patch.

When applied across the input, quantum pooling produces a feature map of size $m \times H_{out} \times W_{out}$, where m is the reduced qubit count. This measurement-driven pooling mechanism not only reduces dimensionality but also provides implicit regularization, as the stochastic nature of quantum measurements helps the model resist overfitting to noise. As a result, quantum pooling plays a dual role: it compresses information hierarchically and simultaneously enhances robustness to uncertainty in RF sensing tasks.

E. Classical Classification Head

After quantum convolution and pooling, the extracted quantum features must be aggregated and transformed into predictions over C activity classes. This is accomplished by a classical classification head, which ensures compatibility with standard optimization routines and provides stable decision-making.

The quantum feature maps generated by pooling are first aggregated across patches and flattened into a single vector $\mathbf{h} \in \mathbb{R}^d$, where d is determined by the number of reduced qubits and the spatial dimensions of the feature map. This flattened vector serves as the input to a sequence of fully connected layers. The first layer expands or compresses $\mathbf{h}$

into a higher-level representation, followed by a non-linear activation function (e.g., LeakyReLU) to introduce model expressivity. A second linear layer maps the intermediate representation into C logits, one for each activity class:

$$\mathbf{y} = W_2\,\sigma\left(W_1\mathbf{h} + \mathbf{b}_1\right) + \mathbf{b}_2,$$

where W_1, W_2 and $\mathbf{b}_1, \mathbf{b}_2$ are learnable parameters, $\sigma(\cdot)$ is the activation function, and $\mathbf{y} \in \mathbb{R}^C$ denotes the output logits.

The use of a classical classification head offers several advantages. First, it enables seamless integration with widely used loss functions such as cross-entropy, which simplifies optimization. Second, it provides robustness to noisy measurements from the quantum layers by leveraging the statistical averaging effects of classical layers. Finally, this hybrid design balances the expressive power of quantum feature extraction with the scalability and maturity of classical deep learning. As a result, the classification head serves as a crucial bridge between quantum processing and practical activity recognition in RF sensing.

Algorithm 1 Quantum Convolution (2D Quanv2d)

Require: Input matrix X of size $m \times n$, kernel size $V \times W$, stride s, quantum circuit QC with n_{qubits}.
Ensure: Quantum feature map Y of dimension $n_{qubits} \times H_{out} \times W_{out}$, where $H_{out} = \lfloor (m-V)/s \rfloor + 1$, $W_{out} = \lfloor (n-W)/s \rfloor + 1$.
for $i := 1$ **to** $m - V + 1$ **step** s **do**
  for $j := 1$ **to** $n - W + 1$ **step** s **do**
    $i' := ((i-1) \div s) + 1$
    $j' := ((j-1) \div s) + 1$
    Extract patch $P \leftarrow X[i \ldots i+V-1,\ j \ldots j+W-1]$
    Flatten P into vector $\mathbf{p}$
    Encode $\mathbf{p}$ into quantum state $|\psi\rangle$
    $Y[:, i', j'] \leftarrow QC(|\psi\rangle)$ ▷ Measure Pauli-Z expectation values of all qubits
  end for
end for

Across both datasets and experimental conditions, the proposed QNN framework consistently outperforms classical baselines, confirming the effectiveness of quantum convolution for RF sensing tasks. Larger quantum circuits (9 qubits) yield higher accuracy than smaller ones (4 qubits), demonstrating the benefit of broader quantum receptive fields in capturing complex spatio-temporal dependencies. Furthermore, robustness experiments show that QNN degrades more gracefully under noise, maintaining significantly higher accuracy than ResNet baselines at low SNR levels.

Taken together, these results indicate that QNN not only provides accuracy gains and parameter efficiency under clean conditions but also extends robustness to noisy and cross-domain RF sensing environments, highlighting their potential as a promising direction for next-generation wireless sensing models.

IV. Experimental Evaluation

A. Dataset Description

To evaluate the proposed quantum convolutional framework, we conduct experiments on two RF sensing datasets: XRF55 and Widar. These datasets correspond to different RF sensing tasks and allow us to assess both temporal activity recognition and spatial robustness.

XRF55 Dataset: The XRF55 dataset [19] is designed for activity recognition using time-series signals. It consists of continuous RF measurements collected from human subjects performing predefined actions in a controlled indoor environment. Each instance corresponds to a fixed-length time window capturing the temporal dynamics of RF responses while a subject performs one of four possible activities. The signals include multiple dimensions such as frequency, phase, and RSSI values sampled across time steps. For our study, the sequences are normalized, segmented into local patches, and encoded into quantum states for QNN processing. A subject-independent evaluation protocol is adopted to ensure generalization to unseen individuals. In addition, the dataset provides a clean and controlled benchmark setting, making it suitable for evaluating the fundamental capability of QNN in modeling temporal RF dynamics before considering more complex cross-domain scenarios.

Widar Dataset: The Widar dataset [20] is designed for human activity and gesture recognition using WiFi CSI. It contains large-scale CSI measurements collected across multiple rooms, users, and environmental conditions, making it a challenging benchmark for cross-domain evaluation. Each sample corresponds to a time window of WiFi CSI responses recorded while a subject performs specific gestures or activities. Compared with XRF55, Widar introduces greater variability due to domain shifts in location and subject diversity. In our experiments, the Widar CSI signals are preprocessed into 2D phase matrices, partitioned into patches, and directly encoded as quantum states. This allows us to evaluate the QNN's robustness under more complex and heterogeneous real-world conditions. Furthermore, the diversity of environments and subjects in Widar provides a realistic testbed for assessing generalization, highlighting the importance of robustness against unseen domains in practical RF sensing applications.

B. Experiment Setup

We evaluate the proposed QNN framework on the XRF55 and Widar datasets introduced above. For both datasets, RF sensing signals are segmented into fixed-length windows, normalized, and partitioned into local patches before being encoded into quantum states.

To investigate the impact of quantum circuit size, we configure the quantum convolutional layer with two different patch dimensions. For 2D convolution, we test window sizes of 2×2 and 3×3, corresponding to 4-qubit and 9-qubit parameterized circuits, respectively. Outputs of the quantum circuits are obtained via Pauli-Z expectation values, which serve as compressed quantum features for subsequent processing. All

models are trained with supervised learning using the Adam optimizer (initial learning rate 0.01, weight decay 1×10^{-4}), cross-entropy loss, batch size of 16, and 50 epochs. We adopt a subject-independent evaluation protocol to ensure that training and testing sets consist of disjoint subjects.

The experiments are conducted on a server equipped with an AMD Ryzen Threadripper 3960X CPU and two NVIDIA RTX A5000 GPUs, running Ubuntu 22.04 with PyTorch and PennyLane for hybrid quantum–classical training and simulation.

C. Experiment Result Analyze

Table I: Classification accuracy (%) on the XRF55 dataset. Comparison between baseline models and QNN-enhanced models with different quantum circuit sizes.

Model	Baseline	QNN (4 qubits)	QNN (9 qubits)
ResNet18	68.8	75.0	**81.2**
ResNet50	65.2	73.3	**78.8**

1) Analysis on XRF55 Dataset Results: Table I summarizes the classification accuracy of QNN and baseline models on the XRF55 dataset. For ResNet18, the QNN with a 3×3 window (9 qubits) achieves the best performance with an accuracy of 81.2%, surpassing both the 2×2 window (4 qubits, 75.0%) and the baseline ResNet18 model (68.8%). Similarly, for ResNet50, the QNN with 9 qubits reaches 78.8% accuracy, outperforming the 4-qubit configuration (73.3%) and the baseline ResNet50 model (65.2%).

These results highlight two key observations. First, QNN-enhanced models consistently outperform their classical baselines, demonstrating the effectiveness of quantum convolution in extracting richer RF sensing features. Even when using the smaller 4-qubit circuits, the QNN already achieves accuracy gains of over 6% compared to ResNet18 and more than 8% compared to ResNet50. This indicates that quantum feature extraction provides tangible benefits even with limited circuit complexity.

Second, increasing the quantum circuit size from 4 to 9 qubits provides noticeable accuracy improvements: +6.2% for ResNet18 and +5.5% for ResNet50. This suggests that larger quantum receptive fields can capture more discriminative spatio-temporal dependencies, resulting in stronger representations for classification. The performance gap also shows that the QNN is able to leverage entanglement among a larger number of qubits to represent correlations that classical convolution kernels may fail to capture efficiently.

Overall, the XRF55 experiments confirm that QNN not only provides consistent accuracy improvements over classical Resnet baselines but also scales effectively with circuit size, striking a balance between parameter efficiency and representational power. These findings establish the potential of QNN as a promising alternative to purely classical architectures in RF sensing activity recognition tasks.

Table II: Classification accuracy (%) on the Widar dataset. Comparison between baseline models and QNN-enhanced models with different quantum circuit sizes.

Model	Baseline	QNN (4 qubits)	QNN (9 qubits)
ResNet18	59.4	63.2	**68.8**
ResNet50	61.8	64.4	**70.2**

2) Analysis on Widar Dataset Results: Table II reports the classification accuracy of QNN and baseline models on the Widar dataset. For ResNet18, the QNN with a 3×3 window (9 qubits) achieves the best accuracy of 68.8%, outperforming both the 2×2 window (4 qubits, 63.2%) and the baseline(59.4%). Similarly, for ResNet50, the QNN with 9 qubits achieves 70.2%, exceeding both the 4-qubit configuration and the baseline.

These results reveal two consistent trends. First, QNN-enhanced models again surpass their classical baselines, demonstrating that quantum convolution remains effective even in more complex and heterogeneous conditions. Although the overall accuracies on Widar are lower than on XRF55 due to stronger environmental variability and domain shifts, QNN still provides accuracy gains of 4-6% over ResNet18 and ResNet50 baselines.

Second, scaling the quantum circuit size from 4 to 9 qubits produces significant improvements: +5.6% for ResNet18 and +5.8% for ResNet50. This indicates that larger quantum receptive fields capture additional discriminative features from the Widar signals, which are characterized by cross-domain variations in users, locations, and environments.

Overall, the Widar experiments confirm that QNN consistently improve upon classical models and exhibit robustness under challenging real-world conditions. The results highlight QNN's potential for handling domain diversity and noisy RF sensing data in large-scale sensing applications.

3) Robustness to Noise: To evaluate robustness, we further test the best-performing model configuration under different noise levels. Figure 2 shows the results on both the XRF55 and Widar datasets.

On the XRF55 dataset, the QNN model achieves 78.8% accuracy without noise, and maintains 74.2% at 15 dB, 71.4% at 10 dB, and 66.2% at 5 dB. Although performance drops with increasing noise, the QNN consistently outperforms the baseline ResNet50, which drops from 65.4% to only 48.8% at 5 dB. This demonstrates that QNN retains stronger robustness to noisy RF sensing signals.

On the Widar dataset, a similar trend is observed. The QNN achieves 70.2% without noise and degrades gracefully to 67.4%, 63.8%, and 58.4% at 15 dB, 10 dB, and 5 dB, respectively. In contrast, the baseline model drops sharply from 61.8% to 44.8% at 5 dB.

These results indicate that QNN provides improved noise tolerance across datasets. The use of quantum convolution appears to enhance feature robustness by capturing redundant spatio-temporal correlations, allowing the model to sustain higher accuracy under adverse conditions.

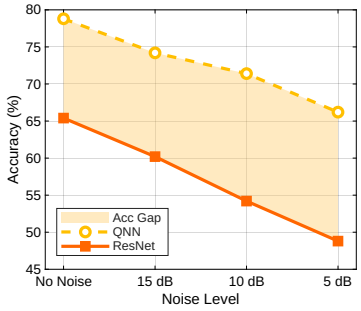

(a) Results on XRF55 dataset.

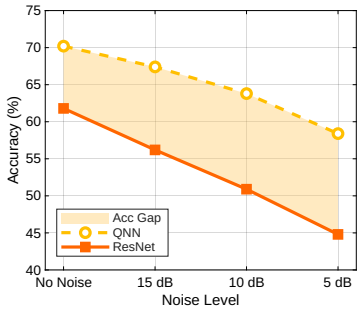

(b) Results on Widar dataset.

Figure 2: Accuracy comparison between QNN-enhanced ResNet50 (9 qubits) and the classical ResNet50 baseline under different SNR levels on (a) XRF55 and (b) Widar datasets.

4) Quantum Advantage Enabled by RF Dataset Characteristics: The substantial performance gains observed on the XRF55 and Widar datasets can be attributed to the intrinsic properties of RF sensing data. RF signals exhibit strong nonlinearity, high-order correlations across time, frequency, and spatial dimensions, and are often affected by phase noise, missing samples, and domain variations such as different users or environments. These complex and distributed patterns are difficult for classical CNNs to fully capture with localized convolution kernels, especially under limited training data or subject-independent evaluation. In contrast, the quantum convolution layer leverages superposition and entanglement to compactly represent high-order spatio-temporal dependencies while maintaining robustness to noise. As a result, QNNs extract more discriminative and noise-resilient features from RF signals, leading to the significantly larger performance improvements observed on both datasets.

V. Conclusion

This paper proposed a hybrid quantum convolutional neural network for RF sensing. By encoding RF signals into quantum states and applying quantum convolutional layers, the framework improves feature extraction with higher parameter efficiency. Experiments show that QNN-enhanced ResNet models outperform classical baselines and maintain higher accuracy under noise. These results highlight QNN as a promising direction for next-generation wireless sensing.

Acknowledgment

This work is supported in part by the NSF under Grants CNS-2319342, CNS-2415208, CNS-2319343, CNS-2415209, IIS-2306789, and IIS-2306791.

References

[1] X. Zhao, L. Wang, Y. Zhang, X. Han, M. Deveci, and M. Parmar, "A review of convolutional neural networks in computer vision," *Artificial Intelligence Review*, vol. 57, no. 4, p. 99, 2024. [Online]. Available: https://doi.org/10.1007/s10462-024-10721-6

[2] T.-X. Tran, N. Q. Khanh Le, and V.-N. Nguyen, "Integrating cnn and bi-lstm for protein succinylation sites prediction based on natural language processing technique," *Computers in Biology and Medicine*, vol. 186, p. 109664, Mar 2025.

[3] X. Hoang Nguyen, V.-D. Nguyen, Q.-T. Luu, T. Dinh Gian, and O.-S. Shin, "Robust wifi sensing-based human pose estimation using denoising autoencoder and cnn with dynamic subcarrier attention," *IEEE Internet of Things Journal*, vol. 12, no. 11, pp. 17 066–17 079, Jan 2025.

[4] B. D. Durtschi and A. M. Chrysler, "Overview of rfid applications utilizing neural networks," *IEEE Journal of Radio Frequency Identification*, vol. 8, pp. 801–810, Oct 2024.

[5] P. Liao, X. Wang, Y. Shan, L. An, and S. Mao, "Wireless sensing in artificial intelligence of things: A general quantum machine learning framework," *IEEE Network*, vol. 39, no. 3, pp. 207–214, Jan 2025.

[6] S. Sajadimanesh, H. Aghaee Rad, J. Paul Latyr Faye, and E. Atoofian, "Nr-qnn: Noise-resilient quantum neural network," *IEEE Access*, vol. 13, pp. 40 185–40 197, Mar 2025.

[7] M. Cerezo, G. Verdon, H.-Y. Huang, L. Cincio, and P. J. Coles, "Challenges and opportunities in quantum machine learning," *Nature Computational Science*, vol. 2, no. 9, pp. 567–576, Jan 2022.

[8] I. Cong, S. Choi, and M. D. Lukin, "Quantum convolutional neural networks," *Nature Physics*, vol. 15, no. 12, pp. 1273–1278, 2019.

[9] M. Schuld and N. Killoran, "Quantum machine learning in feature hilbert spaces," *Phys. Rev. Lett.*, vol. 122, no. 6, p. 040504, Feb 2019.

[10] M. Benedetti, E. Lloyd, S. Sack, and M. Fiorentini, "Parameterized quantum circuits as machine learning models," *Quantum Science and Technology*, vol. 4, no. 4, p. 043001, nov 2019.

[11] J. Biamonte, P. Wittek, N. Pancotti, P. Rebentrost, N. Wiebe, and S. Lloyd, "Quantum machine learning," *Nature*, vol. 549, no. 7671, pp. 195–202, 2017.

[12] E. Peters, J. Caldeira, A. Ho, S. Leichenauer, M. Mohseni, H. Neven, P. Spentzouris, D. Strain, and G. N. Perdue, "Machine learning of high dimensional data on a noisy quantum processor," *npj Quantum Information*, vol. 7, no. 1, p. 161, Mar 2021.

[13] H.-Y. Huang, R. Kueng, and J. Preskill, "Information-theoretic bounds on quantum advantage in machine learning," *Physical Review Letters*, vol. 126, no. 19, p. 190505, May 2021.

[14] S. Jeong, J. Hester, R. Bahr, and M. M. Tentzeris, "A machine learning approach-based chipless rfid system for robust detection in real-world implementations," in *2021 IEEE MTT-S International Microwave Symposium (IMS)*, Jun 2021, pp. 661–664.

[15] Y. Shan, P. Liao, X. Wang, L. An, and S. Mao, "Classical to quantum transfer learning framework for wireless sensing under domain shift," in *GLOBECOM 2023-2023 IEEE Global Communications Conference*. IEEE, 2023, pp. 3167–3172.

[16] T. Koike-Akino, P. Wang, and Y. Wang, "Quantum transfer learning for wi-fi sensing," in *ICC 2022 - IEEE International Conference on Communications*, Aug 2022, pp. 654–659.

[17] S. Mittal, Y. Chand, and N. K. Kundu, "Hybrid quantum neural network based indoor user localization using cloud quantum computing," in *2024 IEEE Region 10 Symposium (TENSYMP)*, Nov 2024, pp. 1–8.

[18] J. Preskill, "Quantum Computing in the NISQ era and beyond," *Quantum*, vol. 2, p. 79, aug 2018.

[19] F. Wang, Y. Lv, M. Zhu, H. Ding, and J. Han, "XRF55: A radio frequency dataset for human indoor action analysis," *Proc. ACM Interact. Mob. Wearable Ubiquitous Technol.*, vol. 8, no. 1, pp. 21:1–21:34, Mar. 2024.

[20] Y. Zheng, Y. Zhang, K. Qian, G. Zhang, Y. Liu, C. Wu, and Z. Yang, "Zero-effort cross-domain gesture recognition with wi-fi," in *Proceedings of the 17th Annual International Conference on Mobile Systems, Applications, and Services*, New York, NY, USA, Jun 2019, p. 313–325.